



## Large Scale Traveling Ionospheric Disturbances during geomagnetic storms in the Australian region

Amol Kishore\*<sup>(1)</sup>, Sushil Kumar<sup>(1)</sup>, and Vickal Kumar<sup>(2)</sup>

(1) University of the South Pacific, Suva, Fiji; e-mail: amol.kishore@usp.ac.fj; sushil.kumar@usp.ac.fj

(2) Space Weather Services Branch, Australian Bureau of Meteorology; e-mail: vickal.kumar@bom.gov.au

### Abstract

Large-scale travelling ionospheric disturbances (LSTIDs) are detected using the critical frequency of the  $F_2$  layer ( $f_oF_2$ ) of the ionosphere. The HF interferometry (HF-Int) technique is applied to the network of ionosondes in the Australian region to detect and estimate propagation parameters. Here we present traveling ionospheric disturbances (TIDs) characteristics (period, velocity, and intensity) associated with selected geomagnetic storms. The TID response during geomagnetic storms varies significantly owing to the differing storm evolution patterns. Results show the morphology of parameters detected continually changes with time corresponding to highly dynamic response effects on the ionosphere. TIDs detected had a wide range of velocity magnitudes (mean  $\pm$  standard deviation) such as  $687 \pm 16$  m/s during onset phase,  $516 \pm 125$  m/s during main phase and  $569 \pm 91$  m/s during the recovery phase of the storm presented here. Propagation directions are predominantly equatorward with east and west deviations owing to higher latitude source generations associated with storm induced intensifications. The HF-Int system uses spectral techniques to estimate the dominant period and outputs the spectral energy contribution (SEC) which is a measure of the contribution of the TID to the total variability of the time series. TID activity levels are based on SEC criteria mostly indicated moderate and weak events with a range of periods 60 – 140 min.

### 1. Introduction

Traveling ionospheric disturbances (TIDs) cause quasi-periodic oscillations of the F-region electron densities with periods from a few minutes to several hours. The density perturbations disrupt navigation, communication and surveillance systems. Large scale TIDs (LSTIDs) often associated with auroral, and geomagnetic storms have most dramatic impacts on such systems. It is therefore important to monitor TIDs and develop understanding of the source of TIDs. Relevant knowledge of relationship between TID properties and TID sources will help improve the interpretation of TID warning systems.

TIDs are manifestations of global scale ionospheric irregularities arising as a response to atmospheric gravity waves (AGW). AGWs are low frequency transverse waves (periods larger than 10 min in the ionosphere) having

frequencies low enough to be affected by gravity. They play an important role in atmospheric dynamics, vertical energy transport, and in particular mesosphere-thermosphere-ionosphere coupling.

During geomagnetic storms there is enhancement of auroral electrojets and intensification of the precipitation of charged particles [6]. Joule heating and Lorentz forces generate AGWs that interacts with the ionosphere causing large scale travelling ionospheric disturbances. Thermospheric waves that interact with the ions in the ionospheric plasma are responsible for the transfer of energy from the high latitudes to the low latitudes. LSTIDs generated in auroral and sub-auroral regions (from both hemispheres) propagate towards equatorial latitudes [5]. The propagation direction of LSTIDs could be explained by the conditions at the source origins. During geomagnetic disturbances enhancement of auroral electrojets produce complex ionization disturbances. These electric currents lie in the horizontal (east-west) direction. When waves are excited by auroral electrojets, TIDs can be thought to be generated in synchronization over great distances along the auroral oval. The constant phase surface of the TID is parallel to the auroral zone over a large longitudinal range and propagate outward towards lower latitudes. The direction of these waves manifested at the lower latitudes are likely due to the variation of the east-west extent of the auroral currents at the generation regions [7]. LSTID properties (periods, velocities and amplitudes) change due to energy dissipation caused by ionic drag, molecular viscosity, and thermal conductivity as they propagate to middle latitudes. At low latitudes their signatures are often mixed with ionospheric disturbances from other factors such as equatorial eastward electrojets, ionospheric irregularities and penetration electric fields associated with storms [3].

We present a method of tracking TIDs during various storm phases and compare the observed variations in propagation parameters with storm development.

### 2. Methodology

The HF-Int technique adopted from [1] have been developed using Matlab codes to produce reports of TID propagation parameters for selected time intervals. The system developed for this work is briefly presented here. The HF-Int system uses timeseries data ( $f_oF_2$ ) from a

network of ionosonde stations over Australian region to detect TIDs. Figure 1 shows the ionosonde network of stations used in the analysis.

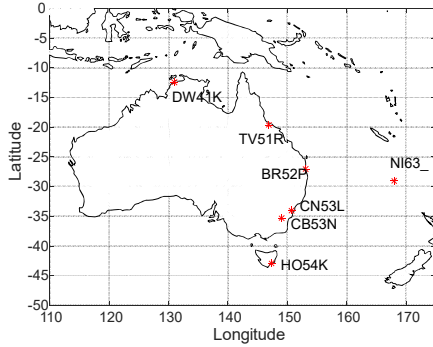


**Figure 1.** Geographic locations of ionosonde stations over Australia (stations are marked with asterisk and are labeled by their URSI station codes).

The system uses spectral and cross correlation techniques to detect and estimate propagation parameters of the observed disturbance. In principle, the system assumes a plane wave propagating disturbances in the horizontal plane and estimates 2D velocity vectors of the detected disturbance at a reference altitude of 350 km corresponding to the F2 region of the ionosphere. In the pre-processing stage 5 min timeseries data is first manually cleaned from outliers and then upsampled to 1 minute interval using linear interpolation resampling technique. The slow varying daily trend is removed by a high-pass digital filter. The remaining residuals contain periods in the range 30 – 180 min associated with disturbances in the range for LSTIDs. In the next stage a six-hour long time window of filtered residual is spectrally analyzed using Lomb-Scargle method at each data point interval for each site of the network. The dominant period is selected for each measurement site as candidate for TID like disturbance. Only sites with coherent periods are considered for further analysis. Finally, cross correlation of the time series residuals is performed between the reference and candidate sites. The propagation parameters are constructed from the measured time delay of the signal. The time delay  $\Delta t_i$  of the disturbance for each station with respect to the reference station is given by:

$$\Delta t_i = \vec{s} \cdot \Delta \vec{r}_i \quad (1)$$

where  $\vec{s} = s_x \hat{i} + s_y \hat{j} = \vec{v}/v^2$  is the slowness vector of the disturbance propagating at velocity  $\vec{v}$ , is an unknown variable;  $\Delta \vec{r}_i = \Delta x_i \hat{i} + \Delta y_i \hat{j}$  is the 2D relative position vector of the  $i^{th}$  station from the reference. For a network of stations with  $i > 3$  the system of equations is overdetermined and is solved by least squares fitting. The velocity vector is obtained using the equation:

$$\vec{v} = \vec{s}/s^2 \quad (2)$$

The system uses stringent selection criteria to register a detection. To minimize ambiguity in the detection process, the system only considers sites with  $\Delta t_i < \pm 60$  min with cross correlation maximum index (CCMi)  $> 0.5$  and periods  $< 30\%$  difference with the reference dominant period. A detection is registered only when there are at least three sites in the network that meet all the criteria and then their propagation parameters calculated.

### 3. Results

#### 3.1. Saint Patrick's Day storm of 17 March 2015

The geomagnetic storm of 17 March 2015 is a widely studied storm in ionospheric studies. A special attention is given to this event because it presents one of the strongest storms of solar cycle 24. The geomagnetic parameters associated with the storm are shown in figure 2.

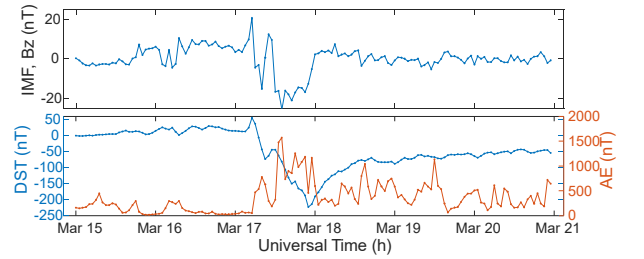


**Figure 2.** Variation of IMF, Bz (top subplot) and Dst and AE index levels (bottom subplot) from 15-20 March 2015.

The storm was associated with a coronal mass ejection resulting in a shockwave that affected the magnetosphere subsequently generating LSTIDs hours later and are observed at mid-latitudes over Australia. Spectral analysis of  $f_oF_2$  timeseries residuals is used to determine periodicity of the disturbances. Figure 3 shows an example of periodograms for each station used in HF-Int to estimate TID characteristics.

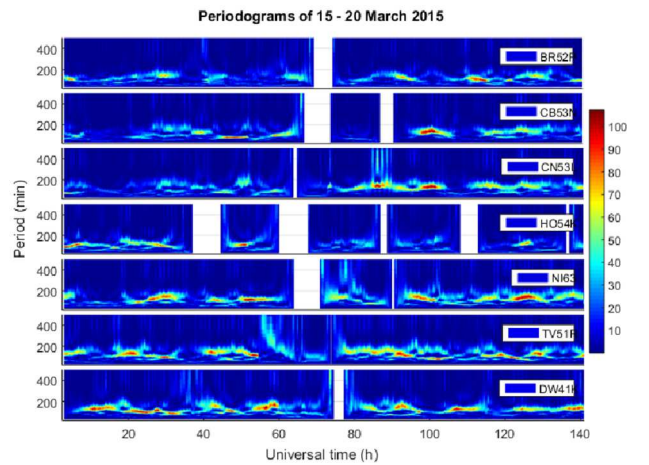


**Figure 3.** Spectral analysis of residuals over Australian network of stations for the storm of 17 March 2015. The color bar represents the spectral power in arbitrary units.

The white patches are due to data gaps or poor-quality data discarded from the analysis.

A TID like disturbance lasting a few hours is seen over Camden, Canberra and Hobart during the onset and main phase of the storm. Figure 4 shows the TID response as temporal variations of propagation parameters (periods, SEC, and velocity) detected at these stations.

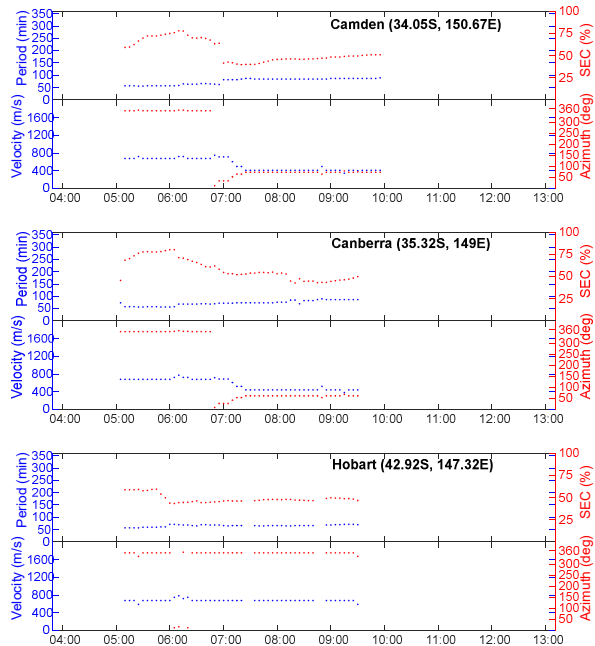


**Figure 4.** Temporal variation of TID propagation characteristics detected during the onset and main phase of the storm of 17 March 2015.

The evolution of TIDs with storm progression shows periods gradually increasing from 57 – 90 min and velocities of 680 m/s initially propagating with an azimuth of 351° and then changing to about 440 m/s with azimuth of 62° over Camden and Canberra.

The corresponding timeseries data plots at Hobart, Camden and Canberra is shown in Figure 5. The plots show quasi periodic variations of  $f_oF_2$  at three ionospheric observatories at latitudes 42.92°S, 35.32°S, and 34.05°S top to bottom series plots respectively. A typical TID progression from higher to lower latitudes are depicted here. The corresponding filtered residuals in the bottom plot show a clearer view of the disturbance progression with latitude.

Moderate to strong TIDs are seen at the mid latitudes during the onset phase of the storm. The activity levels reducing with storm development. During the main phase immediately after the onset TIDs exhibit weaker activity levels with lower velocities and directed northwestward. Another event was registered late in the recovery phase on

20 March 2015. Although the activity levels registered are weak, there is a high detection efficiency with five out of seven stations registering the disturbance with consistent propagation characteristics.

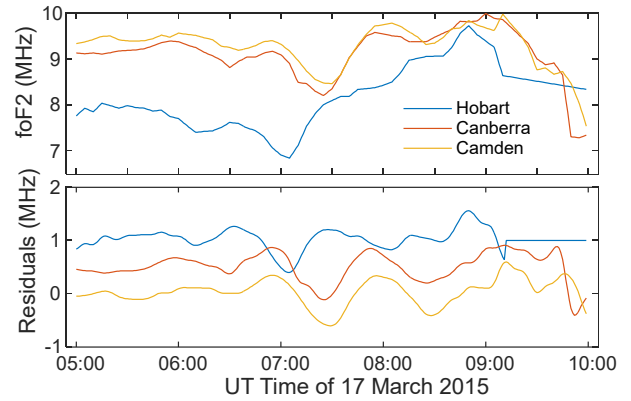


**Figure 5.** Time series  $f_oF_2$  (top) and corresponding filtered residuals (bottom) during disturbance detected on 17 March 2015.

### 3.2. Limitations

HF-Int. uses monostatic measurements from widely spaced network of ionosondes sites. The Australian network of stations are separated by distances from about 700 – 1700 km. This only allows for the detection of LSTIDs with wavelengths greater than these distances. The detection technique assumes a 2D horizontal propagating plane wave. Therefore, parameter estimates only characterize horizontal propagation and do not reveal any information in the vertical direction. HF-Int is sensitive to data quality and data consistency. Data from ionosondes are often subject to system failure, station downtimes, strong sporadic E (Es) and autoscaling errors such as spikes and outliers. Although the data used in this work is manually cleaned by physically removing data spikes and outliers from the time series, long periods of data gaps that do exist reduce detection efficiency since stations without data or incoherent data do not contribute to detection.

### 4. Discussion

The storm of 17 March 2015 produced few TID-like disturbances over Australia. Table 1 shows a comparison of events detected during the storm phases. For this comparison events are selected with cohesive propagation parameters at three or more stations. Lower periods are observed at onset and higher periods late in the recovery phase. All periods have standard deviations less than 10 min showing a good spectral coherence in detections at the different sites. Comparison of propagation velocities show higher velocities during onset compared to the main and recovery phases.

Table 1: Comparison of TID parameters during onset, main and recovery phases of 17 March 2015.

TIDs	Storm of 17 March 2015		
	Onset 05:15 - 06:45 UT (17/3/2015)	Main 07:00 - 09:30 UT (17/3/2015)	Recovery 05:00 - 08:45 UT (20/3/2015)
Period (min) mean $\pm$ std	62.4 $\pm$ 5.3	78.5 $\pm$ 8.3	142 $\pm$ 8.0
Velocity mean $\pm$ std	686.6 $\pm$ 15.8	515.5 $\pm$ 125	568.7 $\pm$ 91.2
Azimuth Range*( $^{\circ}$ )	350.7–353.7	335.4–79.2	322.6–9.2
SEC mean $\pm$ std	64.4 $\pm$ 11.8 (Moderate)	47.4 $\pm$ 3.9 (Weak)	50 $\pm$ 9.3 (Weak)

\*Azimuth is measured clockwise from North, and the range shows the most westward direction to the most eastward direction

The activity levels started moderate and then changed to weak and remained weak at recovery phase. Strong events during storm stages are observed at specific sites lasting few minutes only. Although the storm was one of the most severe geomagnetic storms, the TID response is less impressive with few detections registered. The low detection rate could be attributed to the large number of gaps in the timeseries data. Figueiredo et al. (2017) reported on TID observations over North and South American region during the storm of 17 March 2015. They observed events at 14, 16, 18 and 23 UT with periods of 30 – 50 min and phase speeds of 500 – 700 m/s. Their events showed a northeastward direction in daytime (14 – 19 UT) and northwestward direction at night (23 UT). Velocity estimates detected here are comparable but local daytime and nighttime directions of TIDs are in opposition. It is reasonable to suggest that the TIDs are generated from different locations within the auroral zones and have either eastward or westward enhancements during storm evolution. The higher velocity TIDs observed coincides with the strong southward turning of the IMF-*Bz* and an increasing AE index associated with the onset and early main phase of the storm. The changes in propagation velocity could be associated with atmospheric conditions along the propagation path from high to mid latitudes. The reduction in the propagation velocity and the subsequent change in direction from northeast to northwest is likely due to ion-drag effect and wave energy dissipation during the movement of TIDs from auroral to lower latitudes. Song et al. (2012) suggested that TID damping rate is higher during daytime than nighttime. The onset phase and early main phase of the storm occurs before sunset (10.05 UT) at Canberra thus the first event is observed during the daytime and the arriving waves are slowed due to higher damping at later times. The northwestward propagation direction could be due to the Coriolis forces [3, 8] while the northeastward direction is possibly due to the complex ionospheric convection patterns modified by the development and intensity of the storm [2].

## 5. Summary

During the geomagnetic storm of 17 March 2015, few TID-like events are observed in the Australian region. TID properties change with storm development owing to source generation and propagation conditions. This paper presents a simple approach to understanding the dynamics of TIDs during storm development and provide a small yet significant contribution to the overall quest to understanding the transformations within the magnetosphere-ionosphere system.

## 6. Acknowledgements

Authors are thankful to the University of the South Pacific for supporting the authors to present this paper.

## 7. References

- [1] Altadill D, Segarra A, Blanch E, Juan JM, Paznukhov VV, et al. 2020. A method for real-time identification and tracking of traveling ionospheric disturbances using ionosonde data: first results. *J Space Weather Space Clim* **10**: 2, <https://doi.org/10.1051/swsc/2019042>.
- [2] Astafyeva, E., I. Zakharenkova, and M. Förster. 2015. Ionospheric response to the 2015 St. Patrick's Day storm: A global multi-instrumental overview, *J. Geophys. Res. Space Physics*, **120**, 9023–9037, doi:10.1002/2015JA021629.
- [3] Ding, F., W. Wan, L. Liu, E.L. Aframovich, S.V. Voeykov, and N.P. Perevalova. 2008. A statistical study of large-scale travelling ionospheric disturbances observed by GPS TEC during major magnetic storms over the years 2003–2005. *Journal of Geophysical Research*, Vol. **113**.
- [4] Figueiredo, C. A. O. B., C. M. Wrasse, H. Takahashi, Y. Otsuka, K. Shiokawa, and D. Barros, 2017. Large-scale traveling ionospheric disturbances observed by GPS dTEC maps over North and South America on Saint Patrick's Day storm in 2015, *J. Geophys. Res. Space Physics*, **122**, 4755–4763, doi:10.1002/2016JA023417.
- [5] Hajkovicz, L. A. 1991. Global onset and propagation of large-scale traveling ionospheric disturbances as a result of the great storm of 13 March 1989, *Planet. Space Sci.*, **39**, 583–593.
- [6] Hunsucker, R., 1982. Atmospheric gravity waves generated in the high latitude ionosphere: a review. *Review of Geophysical Space Physics*, Vol. **20**, pp. 293–315.
- [7] Maeda S. & Handa S., 1980. Transmission of large-scale TIDs in the ionospheric F2-region, *J. Atmos. Sol. Terr. Phys.*, **42**, 853–859.
- [8] Song, Q., F. Ding, W. Wan, B. Ning, and L. Liu. 2012. Global propagation features of large-scale traveling ionospheric disturbances during the magnetic storm of 7–10 November 2004, *Ann. Geophys.*, **30**, 683–694, doi:10.5194/angeo-30-683-2012.